Published in final edited form as:
Dev Biol. 2007 July 15; 307(2): 214–226.

The role of the SPT6 chromatin remodeling factor in zebrafish embryogenesis

Fatma O. Kok[1,2], **Emma Oster**[3], **Laura Mentzer**[1], **Jen-Chih Hsieh**[4], **Clarissa A. Henry**[3], and **Howard I. Sirotkin**[1,*]

1*Department of Neurobiology and Behavior, Stony Brook University, Stony Brook, New York 11794*

2*Graduate Program in Molecular and Cellular Biology, Stony Brook University, Stony Brook, New York 11794*

4*Department of Biochemistry, Stony Brook University, Stony Brook, New York 11794*

3*Department of Biological Sciences, University of Maine, Orono, ME 04469-2988*

Abstract

Somitogenesis is a highly controlled process that results in segmentation of the paraxial mesoderm. Notch pathway activity in the presomitic mesoderm is fundamental for management of synchronized gene expression which is necessary for regulation of somitogenesis. We have isolated an embryonic lethal mutation, *SBU2*, that causes somite formation defects very similar to Notch pathway mutants. *SBU2* mutants generate only 6-7 asymmetrically arranged somites. However, in contrast to Notch pathway mutants, these mutants do not maintain previously formed somite boundaries and by 24 hpf, almost no somite boundaries remain. Other developmental processes disrupted in *SBU2* mutants include tail morphogenesis, muscle fiber elongation, pigmentation, circulatory system development and neural differentiation. We demonstrated that these defects are the result of a nonsense mutation within the *spt6* gene. *spt6* encodes a transcription elongation factor that genetically interacts with the Paf-1 chromatin remodeling complex. *SBU2* mutant phenotypes could be rescued by microinjection of *spt6* mRNA and *spt6* morpholinos phenocopied the mutation. Our real-time PCR analysis revealed that Spt6 is essential for the transcriptional response to activation of the Notch pathway. Analysis of *sbu2;mib* double mutants indicates that Spt6 deficiency suppresses the neurogenic effects of the *mib*. Altogether, these results demonstrate that Spt6 is critical for somite formation in zebrafish and suggest that some defects observed in *spt6* mutants result from alterations in Notch signaling. However, additional Spt6 mutant phenotypes are likely caused by vital functions of Spt6 in other pathways.

Introduction

Somites establish the segmental outline of the vertebrate embryo. Bilateral pairs of paraxial mesoderm cells flanking the notochord are first organized into epithelial tissue blocks that then separate from more caudal cells in a regulated fashion, giving rise to highly organized transient structures on the dorsal side of the embryo. These structures then differentiate into dermis of the dorsal skin, vertebrae and skeletal muscles of the trunk and tail.

*Corresponding author: Department of Neurobiology and Behavior, Stony Brook University, Stony Brook, New York 11794, Phone: 631-632-4818, Fax: 631-632-6661, Email: Howard.Sirotkin@sunysb.edu.

The process of somitogenesis is regulated by synchronized expression of Notch pathway components in the presomitic mesoderm (PSM) (Holley et al., 2000; Jiang et al., 2000; Pourquie, 2001; Pourquie, 2003). These include *lunatic fringe* in chick and mouse (Forsberg et al., 1998; McGrew et al., 1998), delta homolog *deltaC* (Jiang et al., 2000) and several *Hairy and Enhancer of Split–Related (Her)* b-HLH repressor genes *her1* and *her7* in zebrafish (Henry et al., 2002; Holley et al., 2000; Holley et al., 2002; Oates and Ho, 2002). Inhibiting the Notch pathway in mice and zebrafish severely disrupts posterior somite formation (Conlon et al., 1995; Evrard et al., 1998; Henry et al., 2002; Hrabe de Angelis et al., 1997; Kusumi et al., 1998; Oates and Ho, 2002; Oka et al., 1995; Takke and Campos-Ortega, 1999; van Eeden et al., 1996; Wong et al., 1997; Zhang and Gridley, 1998).

The first Tubingen large scale genetic screen identified five loci, *fused somites* (*fss*), *beamter* (*bea*), *after eight* (*aei*), *deadlyseven* (*des*) and *white tail/mindbomb* (*wit/mib*), that are required for somite formation in zebrafish (van Eeden et al., 1996). Later, it was shown that four of those genes, *bea*, *aei*, *des*, and *wit/mib*, encode the respective Notch pathway components: notch ligands *deltaC* (Julich et al., 2005), *deltaD* (Holley et al., 2000), notch receptor *notch1a* (Holley et al., 2002) and *mib*, an E3 ubiquitin ligase which is required for cellular localization and activity of Delta (Itoh et al., 2003). The absence of posterior somites is a characteristic phenotype observed in all of the Notch pathway mutants. After forming 1 to 9 anterior somites, segmentation of the posterior PSM is interrupted and no new somites are formed (van Eeden et al., 1996).

In a genetic screen to isolate mutations disrupting neural patterning and embryogenesis, we identified an embryonic lethal mutation, *SBU2* that has somite defects resembling Notch pathway mutants. In particular, *SBU2* mutants only form 6-7 anterior somites. In addition, *SBU2* embryos have other phenotypes including defects in muscle fiber differentiation, pigmentation, circulatory system development and neural differentiation. RNA *in situ* hybridization with mesodermal markers revealed that *SBU2* mutants have reduced paraxial mesoderm and little lateral plate mesoderm. However, intermediate mesoderm is largely unaltered suggesting that not all mesodermal subtypes are disrupted by the *SBU2* mutation. While early regional neural makers are expressed in *SBU2*, many markers for differentiated neurons and neural crest are absent.

Using positional cloning, we identified a mutation that produces a premature stop codon within the *spt6* gene. The *SBU2* defects could be rescued by microinjection of *spt6* mRNA into *SBU2* mutant embryos. Microinjection of *spt6* morpholino oligonucleotides phenocopied the *SBU2* phenotype. Together, these results demonstrated that the *SBU2* phenotypes are produced by disruption of the *spt6* locus. The *pandora*^{m313} (*pan*) mutation was previously shown to disrupt the *spt6* locus (Keegan et al., 2002). Since *SBU2* is allelic to pan^{m313}, we designate our allele *pan*^{SBU2}. The phenotypes of *pan*^{SBU2} mutants are apparent at an earlier stage and are more severe than the *pan*^{m313} mutants. This finding demonstrates a broader and earlier requirement for Spt6 in zebrafish embryogenesis then was apparent from characterization of *pan*^{m313}.We present evidence that the phenotypic variations between the two spt6 alleles are the result of genetic background differences.

Spt6 was identified in *Saccharomyces cerevisiae* as a transcription elongation factor which interacts with histone H3 and H4 (Bortvin and Winston, 1996). Spt6 functions in chromatin disassembly. During transcription, Spt6 allows RNA pol II to pass through the DNA template and re-establishes chromatin structure after RNA pol II passage (Adkins and Tyler, 2006; Hartzog et al., 1998; Kaplan et al., 2003; Saunders et al., 2003; Swanson and Winston, 1992). Hence, Spt6 is required for persistent yet regulated transcription processes in the cell.

In *C. elegans*, EMB-5, the ortholog of yeast Spt6, genetically interacts with LIN-12 (Notch family transmembrane receptor) (Hubbard et al., 1996). EMB-5 augments the penetrance of LIN-12 related defects on vulval morphology. Furthermore, interactions between the ankyrin repeats of EMB-5 and both LIN-12 and GLP-1 were detected in yeast two-hybrid analysis. These findings suggest that EMB-5/Spt6 might function in modulation chromatin structure upon activation of LIN-12/Notch pathway and regulate transcription of Notch pathway genes (Hubbard et al., 1996).

In *spt6* mutants, we found that activation of target genes by ectopic expression of Notch was suppressed. However, analysis of *mindbomb;SBU2* double mutants demonstrated that the neurogenic phenotype in *mindbomb* mutants is suppressed by mutation of Spt6. While the *pan*^{SBU2} phenotype establishes that Spt6 is broadly required for many aspects of development, we also observe somite defects characteristic of Notch mutants. These studies provide the first evidence for a role for Spt6 in Notch signaling in vertebrates. In addition, we demonstrate a specific developmental requirement for the Spt6 transcription elongation factor in somitogenesis in zebrafish.

Results

Identification of a mutant with disrupted somitogenesis

We performed a haploid ENU mutagenesis screen to identify mutations affecting zebrafish embryogenesis. In *SBU2* mutant embryos only 6-7 anterior somites form and further segmentation is severely interrupted (Fig. 1). *SBU2* embryos also have a short body length and slightly wide notochord and neural keel which may result from defects in convergence and extension movements. In addition, other defects including tail elongation, anterior neural, circulatory, and pigmentation defects are apparent in *SBU2* mutant embryos. After about 20 hrs, many of the previously formed structures start to deteriorate (Fig. 1J).

The *SBU2* somite defects resemble the Notch pathway mutants. Embryos obtained from *SBU2* intercrosses do not show any morphological abnormalities during gastrulation (data not shown). During early somitogenesis, *SBU2* homozygous embryos can be distinguished from their siblings due to their indistinct and irregularly placed somite boundaries (Fig. 1A-A' and 1B-B'). At 4-5 somite stage, altered somite boundary formation is evident in *SBU2* embryos (Fig. 1D-D'). By the time their heterozygous or wild-type siblings reach the 10-13 somite stage, homozygous *SBU2* embryos exhibit only irregularly and asymmetrically formed 6-7 anterior somites (Fig. 1F-F' and 1H-H'). After that stage, somitogenesis stops in *SBU2* mutants. In most *SBU2* mutants, previously formed somite boundaries start to degenerate around 4-5 somite stage leaving either incomplete or no somite boundaries by 24 hours post-fertilization (hpf) (Fig. 1J).

Mesodermal gene expression is disrupted in *SBU2* mutants

During somitogenesis, the paraxial mesoderm is segmented into highly arranged tissue blocks. Since *SBU2* has segmental defects, we examined the effects of the mutation on specification of mesodermal cells. As somites are specifically derived from paraxial mesoderm cells, we first studied the state of differentiated paraxial mesoderm cells in *SBU2* embryos. RNA *in situ* hybridization with paraxial mesodermal markers *papc* and *spt* revealed that *SBU2* mutants have a reduced expression domain of paraxial mesoderm markers in the A-P dimension (arrowheads, Fig. 2A-D). In addition, the boundaries of the expression domain are less distinct in SBU2 mutants. However, this observation does not explain the somitogenesis defects observed in *SBU2*, since *tri; kny* double mutants form very little paraxial mesoderm but somite boundaries still form (Henry et al., 2000).

Rostrocaudal polarity of the somites is also disrupted in SBU2 mutants. The segmental expression of myoD in the posterior half of the somites (Weinberg et al., 1996) is lost (Fig. 2E-F) whereas gene expression at anterior half of the somites such as papC (Yamamoto et al., 1998), ephB2 (Durbin et al., 1998) and dld (Holley et al., 2002; Jiang et al., 2000) is reduced and diffuse (Fig. 2A-B, G-H and 3I-L) in SBU2 mutants. Although muscle differentiation is disrupted and myoD expression is completely lost in lateral paraxial mesoderm, adaxial cell specification is less severely disrupted (Fig. 2E-F).

We also studied differentiation of the other subdivisions of the mesodermal precursors such as lateral plate mesoderm and intermediate mesoderm. An early erythroid lineage marker, *gata-1* (Tsai et al., 1989) is not expressed in *SBU2* embryos (Fig. 2I, J) suggesting that lateral plate mesoderm in *SBU2* embryos is severely disrupted by the 10 somite stage. *SBU2* embryos have additional defects in lateral plate mesoderm as evidenced by the failure of heart tube formation (data not shown). However, RNA *in situ* hybridization with the nephrogenic marker *pax2a* (Krauss et al., 1991) reveals no difference between wild type and *SBU2* embryos (Fig. 2K, L). This suggests that there is no defect in differentiation of intermediate mesoderm. Together these results suggest that the mutation underlying the *SBU2* phenotype disrupts somite formation, specification of paraxial and lateral plate mesoderm but intermediate mesoderm is relatively unaffected.

The segmentation of the PSM is regulated by the periodic expression of genes including *her1*, *her7* and *deltaC* and disruption of these genes causes somitogenesis defects (Gajewski et al., 2003; Henry et al., 2002; Holley et al., 2002; Jiang et al., 2000; Oates and Ho, 2002). To ascertain whether periodic gene expression is altered in *SBU2*, we assayed expression of these markers (Fig. 3A-L). Distinct stripes of *her1* and *her7* are observed in wild-type embryos at both the 3 and 10 somite stages. However, in *SBU2* mutants, stripes of *her1* and *her7* are present but exceedingly reduced (arrows, Fig. 3A-H). This shows that expression of molecular clock components is disrupted at early stages of somitogenesis in *SBU2* mutants and the loss of molecular clock components correlates with the onset of the segmentation defects. The domain of *papc*, which is expressed more proximal to somite boundary formation, is spatially disrupted. Thus, it is possible that low levels of periodic gene expression may fail to properly specify expression of downstream genes such as *papc* that are critical for somite boundary formation (Yamamoto et al., 1998). Expression of another Notch pathway gene *deltaD* is also reduced but more diffuse in *SBU2* mutants (arrows, Fig. 3I-L). Similarly, the expression of tbx24, which is required for PSM maturation (Nikaido et al., 2002) is reduced in SBU2 mutants (Fig 3M-P). These results indicate that somite segmentation as well as PSM maturation is highly disrupted in *SBU2* mutants. Muscle differentiation may also be disrupted, as expression of the myogenic regulatory factor MyoD is absent in lateral paraxial mesoderm (Fig. 2F).

Somite boundaries deteriorate in *SBU2* mutants

SBU2 mutants have segmentation defects very similar to Notch pathway mutants. To further characterize these defects in *SBU2* embryos, we examined the somite structure of 29 somite stage *SBU2* mutant embryos using a series of antibodies. Focal adhesion kinase (Fak) is robustly accumulated at somite boundaries during somitogenesis and persists at these boundaries (Henry et al., 2001; Hens and DeSimone, 1995; Polte et al., 1994) (arrows, Fig. 4A, A'). In 29 somite stage *SBU2* mutants, Fak fails to accumulate at somite boundaries, even in the anterior of the embryos (Fig. 4B, B'). This observation is unexpected, since anterior somite boundaries formed earlier in development morphologically. Therefore, we conclude that somite boundaries that form are not maintained properly in *SBU2* mutants. This result differs from Notch pathway mutant embryos in which irregular posterior somite boundaries eventually form, albeit later in development compared to wild-type embryos (Henry et al., 2005). Thus, the initial somite phenotype of *SBU2* and Notch pathway mutant embryos is

similar, but the later boundary phenotype of *SBU2* is more severe compared to previously characterized Notch pathway mutants.

It has been hypothesized that migrating slow muscle fibers mediate the belated formation of boundaries in fss-type mutant embryos (Henry et al., 2005; Julich et al., 2005). In *SBU2* mutant embryos, boundaries do not form even later in development. We therefore asked if slow muscle fiber morphology is disrupted in *SBU2* mutant embryos. Staining with the slow muscle antibody F59 revealed a reduced number of differentiated slow muscle fibers in *SBU2* mutants (Fig. 4C, D). Furthermore, the initial segmental defects in these embryos are reflected in slow fiber organization; slow fibers are not as well organized as in wild type embryos. In addition, slow muscle fiber staining becomes fainter and gradually fades away in the posterior (Fig. 4C', D'). This result is not surprising because small gaps in adaxial (slow muscle precursor) *myoD* expression (Fig 2F) suggest that there may be fewer slow muscle precursors present in *SBU2* embryos which fail to properly differentiate into muscle fibers. The disruption in slow fiber organization at 29 somites in *SBU2* is more severe then that of Notch pathway mutants. In both the Notch pathway mutant embryos *aei/deltaD* and *des/Notch1*, slow muscle fiber morphology is disrupted early but later recovers (Henry et al., 2005).

Clearly, slow-twitch muscle fiber development is disrupted in *SBU2* mutant embryos. Analysis of *myoD* expression suggests that there might also be a fast muscle defect (Fig. 2F). We utilized an antibody against β-catenin that visualizes all cells to ask if fast muscle morphogenesis is disrupted in *SBU2* mutant embryos (Topczewska et al., 2001). In wild-type embryos, the expression and lateral displacement of slow muscle fibers correlates with fast MyHC expression and muscle cell elongation (Blagden et al., 1997;Cortes et al., 2003;Henry and Amacher, 2004). Fast muscle cell elongation is disrupted throughout the axis of *SBU2* mutant embryos. Anteriorly, some cells elongate but elongation is inconsistent and disorganized (Fig. 4F). Posteriorly, fast cell elongation is also disrupted (Fig. 4F'). The disruption of fast muscle fiber formation in *SBU2* mutant embryos was confirmed by analysis of myosin light chain (MLC) expression. Whereas fibers in wild-type embryos express significant amounts of MLC, protein is undetectable in SBU2 mutant embryos (Figure 4H-H'), Taken together, these data indicate that muscle morphogenesis is more severely disrupted in *SBU2* mutant embryos than in Notch pathway mutant embryos.

SBU2 mutants have neural defects

Lateral inhibition mediated by Notch signaling regulates neuron number in both vertebrates and invertebrates. In *Drosophila*, Notch pathway mutants are neurogenic. In zebrafish, ectopic neurons or neural progenitors are readily apparent in *mib* (Jiang et al., 1996; Schier et al., 1996). However, the neurogenic defects in *des* and *aei* are more subtle (Gray et al., 2001; Holley et al., 2000). To determine whether *SBU2* embryos are neurogenic, we performed in-situ hybridization with neural markers. RNA *in situ* hybridization with midbrain-hindbrain boundary and placode marker, *pax2a* (Krauss et al., 1991) revealed that placode formation is delayed (arrowheads, Fig. 5D). The overall midbrain-hindbrain boundary and placode expression of *pax2a* is reduced but the general spatial pattern of *pax2a* is largely unaffected in *SBU2* embryos (Fig. 5B, D). However, the midbrain-hindbrain boundary is not morphologically apparent in living embryos (Fig 1J). This suggests that although these cells initiate proper gene expression at the midbrain-hindbrain, the boundary does not form. Similarly, expression of the hindbrain marker *krox20* (Oxtoby and Jowett, 1993) is also delayed in *SBU2* embryos. However, as development progresses, *krox20* recovers and the overall pattern becomes similar to that of wild type embryos (Fig. 5E-H).

The neural marker *huC*, reveals the number of the differentiated neurons in zebrafish embryo during development (Kim et al., 1996). *SBU2* embryos express very little, if any, *huC* (Fig. 5I-I' and 5J-J'). Similarly, epibranchial neuron marker, *phox2a* expression is weak or completely

absent in *SBU2* embryos (data not shown). Together these data indicate that *SBU2* embryos generate few differentiated neurons and are not neurogenic. In zebrafish, somitogenesis is more sensitive to disruptions in notch signaling than neurogenesis as evident by the weak neurogenic phenotype in *des* (Gray et al., 2001). Potential neurogenic effects of *SBU2* may be masked by additional requirements for the protein in neurogenesis. Alternatively, *SBU2* might not influence Notch-mediated lateral inhibition in neural tissue.

Disruption of *spt6* causes the *SBU2* phenotype

To identify the gene that is responsible for the *SBU2* phenotype, a large genetic mapping panel comprising 6928 meioses was assembled. *SBU2* was mapped to a ~5 cM interval in the centromeric region of linkage group 21 between Z7809 and Z10432 Because of the proximity to the centromere, recombination is suppressed in this region. Therefore, the genetic distance corresponds to a larger then average physical distance. Using the sequence information from the Sanger Ensembl genome assembly (www.ensembl.org/Danio_rerio) a series of polymorphic markers was generated to narrow the interval (Fig. 5A). Sequence analysis of the genes at that region revealed a C to T transition at nucleotide 3931 of the coding sequence of the *spt6* gene (Fig. 6B, bottom panel). This sequence change was detected in 75/75 mutants analyzed using restriction analysis of a PCR product generated from the locus (see Materials and Methods). 0/95 phenotypically wild-type sibling were homozygous for the sequence change. This mutation creates a premature stop codon in exon 30 (Fig. 6B). The truncated Spt6 protein lacks the C-terminal 415 amino acids which includes a Src homology 2 domain important for recognition and binding to phosphorylated tyrosine (Pawson, 1995) (Fig. 6C).

To confirm that disruption of the *spt6* gene produces the *SBU2* phenotype, we assayed the ability of *spt6* mRNA to rescue the *SBU2* phenotype and determined whether microinjection of morpholinos directed against *spt6* phenocopy the *SBU2* mutants. *spt6* mRNA was injected into embryos from a *SBU2* heterozygote intercross. Overexpression of *spt6* sense mRNA in *SBU2* mutants rescues most of the somitogenesis and tail elongation defects (compare Fig. 6E and 6G). Overexpression of *spt6* mRNA doesn't produce an effect on wild type embryos (data not shown).

Next, we designed a morpholino antisense oligonucleotide to span the boundary between the 30th exon and 30th intron of *spt6*. *spt6* morpholino binding to the *spt6* pre-mRNA is predicted to create a missplicing event that deletes exon 30 and causes a frameshift mutation. The protein transcribed from that misspliced *spt6* RNA is predicted to closely mimic the Spt6 protein structure in *SBU2* mutants. Injection of *spt6* morpholino into genotypically wild-type siblings of *SBU2* mutants results in embryos that strongly resemble the *SBU2* phenotype (compare Fig. 6E and H). Based on linkage, sequence change, rescue and morpholino experiments; we conclude that disruption of *spt6* results in the *SBU2* phenotype.

An *spt6* mutation was previously shown to be the cause of the *pandora* phenotype (Keegan et al., 2002). The genetic lesion in *pan* produces a truncated protein of 829 amino acids. We think that both mutations likely produce non-functional proteins. *pandora* mutants exhibit defects in cardiac differentiation, pigmentation and ear formation. However, stronger defects in these cell types are also observed in *SBU2* mutants (data not shown). A complementation test was performed to determine if the two mutations are allelic. Since the two mutations fail to complement, we designate our allele as pan^{SBU2}. In some crosses pan^{m313}/pan^{SBU2} embryos resemble pan^{m313} mutants and in others pan^{SBU} mutants (data not shown). This result suggest that genetic background strongly influence the *spt6* mutant phenotype. In addition injection of the *spt6* morpholino into some wild-type stocks produces a phenotype (Fig. 6I) more similar to pan^{m313} (Fig. 6F) than pan^{SBU2} (Fig. 6E). Therefore, we conclude that the phenotypic differences between pan^{m313} and pan^{SBU2} most likely stem from genetic background differences and not from difference in properties of the alleles.

Notch signaling is suppressed in *SBU2* mutants

Since the somite defects in *spt6* mutants resemble Notch pathway mutants, we sought to determine whether Spt6 is required for activation of the Notch pathway. We activated the Notch pathway by microinjection of mRNA corresponding to the intracellular domain of the Notch protein (NICD) into *SBU2* embryos and measured transcript levels of Notch target genes at the 10-somite stage (Fig. 7A-C). As expected, activation of Notch pathway induced transcription of Notch pathway target genes, *her1*, *her6*, *her7* (Fig. 7A-C,). Conversely, homozygous *SBU2* mutants have reduced levels of those transcripts (Fig. 7A-C,). This observation is consistent with what was observed in the RNA *in situ* hybridization analysis of SBU2 (fig 2E-H). However, induction of target genes by the *NICD* mRNA was suppressed in *SBU2* mutant embryos (Fig. 7A-C). It should be noted that disruption of Spt6 function in *SBU2* embryos does not have same effect on every Notch target gene. *her6* transcript levels are not highly affected by disruption of Spt6 function while *her1* and *her7*, two essential Notch target genes for somite formation, are clearly suppressed. These results demonstrate that Spt6 is required for proper response to Notch activation.

Genetic interactions between Spt6 mutation and *mindbomb*

The Notch pathway regulates somitogenesis in zebrafish embryos by controlling the synchronous gene expression at the PSM. Mutation of Notch pathway genes leads to characteristic posterior somite defects (van Eeden et al., 1996) very similar to *SBU2* mutants. This suggests that Spt6 might have a function in the Notch pathway in regulation of somite formation. Previous studies also indicate a genetic interaction between the *C. elegans* homologue of Spt6, EMB-5 and the *C. elegans* notch homologues LIN-12/GLP-1 (Hubbard et al., 1996). To determine whether mutation of Spt6 enhances the phenotype of Notch pathway mutants in zebrafish, we generated *mib;SBU2* double mutants. *mindbomb* (*mib*) is an E3 ubiquitin ligase required intracellular localization of the Notch ligand Delta. The overall somite morphology and body shape of the double mutants resembled *SBU2* single mutants (Fig. 8A-D). The somite defects caused by disruption of Spt6 is not enhanced by *mib* mutation.

To determine if mutation of spt6 enhances the neurogenic phenotype of *mib*, we performed RNA *in situ* hybridization with a *huC* probe on the double mutants. We observed decreased numbers of *huC* positive cells in *mib;SBU2* double mutants compared to *mib* single mutants (Fig. 8E-H). The number of *huC* positive cells in the double mutant was less than in wild-type embryos but more then in *SBU2* single mutants (Fig. 8E-H). Disruption of Spt6 does not enhance the neurogenic defects in Mib but instead largely suppresses them. These findings suggest that Spt6 is not required for Notch mediated suppression of neurogenesis.

Discussion

We identified and characterized an embryonic lethal mutation, *SBU2*, which gives rise to somite abnormalities in zebrafish embryos. These defects are similar to, but more severe than Notch mutant embryos suggesting that additional pathways require SBU2. *SBU2* mutants are characterized by severe posterior segmentation and differentiation defects, disruption of gene expression in paraxial and lateral plate mesoderm, but intermediate mesoderm is unaffected. Moreover, although the patterns of many early regional neural markers in the mutant embryos are not severely altered, later, neural differentiation is highly disrupted. We utilized mRNA rescue and morpholino knockdown experiments to demonstrate that the phenotype observed in *SBU2* mutant embryos is due to disruption of the *spt6* locus. Altogether, our studies indicated that Spt6 has important functions during early patterning and somitogenesis of the zebrafish embryo.

Relationship of *SBU2* and *pandora*

A mutation that disrupts splicing of *spt6* and is predicted to give rise to a truncated protein was shown to give rise to *pan* phenotype (Keegan et al., 2002). Complementation studies between *SBU2* and *pan* confirmed that the two mutations are allelic. In *pan*^{m313} mutants, however, the truncated Spt6 protein is predicted to be much shorter than the protein produced in *SBU2* mutants. The Pan^{m313} protein lacks the S1 RNA binding domain in addition to the SH2 domain. Given the function of Spt6 as a modulator of chromatin structure, the absence of the S1 nucleic acid binding domain in *pan* is consistent with the loss of function of the Spt6 protein. On the other hand, Spt6 protein produced by *pan*^{SBU2} which lacks only the SH2 domain might also fail to interact with other proteins in the transcription elongation machinery. Although both of the *spt6* alleles likely encode non-functional proteins, the phenotypic differences caused by those mutations are very striking. *SBU2* mutants reveal a much earlier and stronger phenotype than *pan* mutants and die around 2 dpf while *pan* embryos display defects much later and usually survive more than 7 days. Moreover, microinjection of *spt6* morpholino can phenocopy *pan*^{SBU2} or *pan*^{m313} depending on the background of the injected embryos (Fig 6). In addition *pan*^{m313}/*pan*^{SBU2} embryos may resemble *pan*^{m313} or *pan*^{SBU}. These observations suggest that severity of the defects in *spt6* mutants is highly genetic background dependent and variations in levels of maternal Spt6 protein may to some degree impact the extent of the defects observed. Similarly, yeast are sensitive to SPT6 copy number (Clark-Adams and Winston, 1987).

Relationship of Spt6 to the Notch pathway

Spt6 protein has been studied in human, mouse, zebrafish, Drosophila, *C. elegans* and yeast. It has been shown to interact with many components of the transcriptional machinery. In yeast, Spt6 protein has ATP-independent nucleosome assembly function, controlling transcription of various sets of genes by modulating the assembly state of the nucleosomes during active transcription (Bortvin and Winston, 1996). In addition *spt6* mutations can suppress the effects of the mutations affecting the Snf/Swi chromatin remodeling complex in yeast (Malone et al., 1993). Similarly, in Drosophila, it was shown that Spt6 protein is associated only with the active form of RNA pol II and has a role in regulation of transcription (Kaplan et al., 2000). Moreover, human SPT6 antagonistically interacts with histones as well as the transactivator domain of human cytomegalovirus pUL69 to modulate transcription (Winkler et al., 2000). Overall, Spt6 is a part of transcription elongation machinery and regulates the transcription of corresponding genes by modulating the chromatin structure in the cell in wide range of organisms. However, in *C.elegans*, EMB-5, a homolog of yeast Spt6, was characterized as a regulator of timing of the gut processor division during gastrulation and controller of oogenesis and required for specific synchronous cell division timing of E cells (Nishiwaki et al., 1993).

Many of the Notch pathway components found in invertebrates are conserved in vertebrates as well (reviewed in (Greenwald, 1998). Our work provides further evidence that Spt6 function is also conserved in a vertebrate model and suggests that it interacts with complexes containing the Notch ICD. An interaction between the *C. elegans* homolog of Spt6, EMB-5 and ankyrin repeats of the LIN-12 and GLP-1, Notch family transmembrane receptors (Hubbard et al., 1996) was identified through yeast 2-hybrid assay. Moreover, when *emb-5* function is eliminated from the *lin-12* mutant embryos, the penetrance of the *lin-12* phenotype is enhanced whereas penetrance of the constitutively active *lin-12* phenotype is reduced. In addition, *emb-5* is required for the proper germline development regulated by *glp-1* (Hubbard et al., 1996). Ectopic activation of *glp-1* cannot rescue the phenotype caused by *emb-5* mutation (Hubbard et al., 1996) indicating that *emb-5* is epistatic to *glp-1*. These observations also suggest that there is a direct functional interaction between e*mb-5* and *lin-12/glp1*.

A recent study also supports the functional interaction between Spt6 and Notch pathway in Drosophila (Tenney et al., 2006). Rad-6/Bre1 histone modification activity is essential for

transcription of Notch target genes (Bray et al., 2005). Paf-1 complex is required for this activity (Wood et al., 2003). Knocking-down Rtf-1, a component of the Paf-1 transcription elongation complex, in N^{nd-1} notch mutant background enhances the phenotype of the notch mutation. Furthermore, the zebrafish homolog of the yeast Rtf-1 protein was recently shown to be disrupted in a novel zebrafish mutant, *white zebra (wze)* (T. Akanuma and S. Takada, personal communications). *wze* also exhibits segmentation defects similar to Notch pathway mutants and pan^{SBU2}.

Since genetic studies indicate that Spt6 interacts with Rtf-1 (Costa and Arndt, 2000), there is a strong possibility that Spt6 also functions in Notch signaling along with Paf-1/Bre1 transcription elongation complex. Other studies (reviewed in (Tsukiyama and Wu, 1997)) support the requirement for appropriate chromatin modifying and remodeling functions for proper transcription of particular genes. In this study, we demonstrated that the response to ectopic Notch activation requires Spt6 function. However, it should be noted that disruption of Spt6 function does not have the same effect on every Notch target gene. We observed much stronger effects on her1 and her7 which are required for proper somite formation, then on her6. Likewise, mutation of Spt6 did not enhance the neurogenic phenotype of *mib*.

In addition to playing a role in Notch signaling, other cellular processes are affected by *spt6* mutation since the overall pan^{SBU2} phenotype is much more severe and complex than Notch pathway mutants. Several signaling pathways including FGF and Wnt are required for posterior development. Some of the defects in pan^{SBU} may stem from defects in these pathways. Most of the Notch pathway mutants can be raised to adulthood indicating that the somitogenesis defects observed in those embryos improve later in development however in pan^{SBU2} mutants, defects become much worse; even the previously formed structures cannot be maintained, and embryos eventually deteriorate and die. Although *spt6* is required for segmentation of the paraxial mesoderm in the zebrafish embryo, it is also required for many other basic cellular functions. While chromatin remodeling factors like Spt6 have broad cellular roles, they also may be required for specific signal transduction pathways and regulate specific developmental processes.

Materials and methods

Fish husbandry and mutagenesis

Adult zebrafish strains and embryos obtained from natural crossings were maintained at 28.5° C. Developmental stages of the embryos were determined according to Kimmel *et. al*. (Kimmel et al., 1995). For mutagenesis, adult fish were placed in 3.0 mm ENU for 1 hour, once a week for three weeks.

Positional mapping of SBU2

Genomic DNA extractions and PCR conditions were performed as described in (Gates et al., 1999). SSLP primers were designed using the zebrafish SSR program (http://danio.mgh.harvard.edu). PCR products were electrophoresed on 3% MetaPhore (Cambrex, Rockland, ME) agarose gels. New polymorphic marker sequences were:

scaf1051ssr7	F: GCCAGTAAATTTTGGCCTTG
	R: GACGTGTGAAGCTGCAGAAA
baczk17e16ssr1	F: ACTGTGCTCTGATGCCTCCT
	R: TGCAAAAATAAGCAAATAAACAAA
baczk17e16ssr3	F: CATTCCGAAATGACCCAGTT
	R: GCCTTTGATTATGTCTGTAAAAGC
baczk17e16ssr5	F: CACAACAACCAACCGCTCTA
	R: CGCAGTACTGAAGACGCAAA
baczk54m16ssr	F: GCCTCGTCCCTACAAACAAA
	R: AACCGCTTGGTATGCTGAAC

paczkp6a12ssr	F: CAAACAACAACTGGGCACTTT R: AGATCCAGATCCGGCTTGA
paczkp6a12snpf	F: CACAAAGGAGATGTCATGCTG R: GCAAGACTTTAACACTGCTACCAGAC
scaf1767ssr8	F: GTGCAGGCCTTGGTGTGTAT R: AAGGTTACCATAAGCCATTAACAA
baczk220h13	F: CAGGTATTTTCCTACACTAACAACAC R: AATTGCCAGATGAAACATGC
bacfin612ssr	F: ACATCCACACAGCCACTCAT R: GGGGTGTAATGGTACACTGGA

Expression constructs, mRNA synthesis and morpholinos

spt6 and myc-*NICD* expression constructs were kindly provided by Deborah Yelon and Scott Holley and generation of these constructs is previously described (Keegan et al., 2002; Takke et al., 1999).

Capped sense mRNA was synthesized using mMESSAGE mMACHINE Kit (Ambion, Austin, TX). Splice morpholino that targets 30th exon-intron boundary of the *spt6* pre-mRNA blocking the proper nuclear processing is designed and synthesized by Gene Tools. The sequence of the morpholino used is 5'-GCCATAGGAACAGCTCACCTCAGTG-3'. Standard control oligo (Gene Tools, Philomath, OR) is used as control. mRNA and morpholino solutions were diluted to desired concentration with 0.2 M KCl supplemented with phenol red. Typically, 100 pg of *spt6* mRNA, 500 pg of *NICD* mRNA and 10 ng of *spt6* splice morpholino is injected to one- to two-cell stage embryos.

Whole mount in-situ hybridization and immunohistochemistry

In situ hybridizations were performed according to Thisse et. al. (Thisse et al., 1993). Digoxigenin labeled probes for *in situ* hybridization were synthesized using T7, T3 or Sp6 RNA polymerase (Roche, Indianapolis, IN). Hybridized probes were detected using NBT/BCIP system (Roche, Indianapolis, IN). Stained embryos were re-fixed in 4% PFA and either stored in 100% methanol or cleared in Benzyl benzoate/benzyl alcohol solution (2:1) and mounted in Canada balsam/methyl salicylate (2.5% v/v) or flat mounted in 70% glycerol. Embryos were viewed with Zeiss Axioplan microscope, digitally photographed with Zeiss Axiocam camera. Images were processed and assembled with Zeiss Axiovision and Adobe Photoshop.

β-catenin, Fak, and F59 staining were performed as previously described (Henry et al 2001; Topczewska et al., 2001; Henry and Amacher, 2004). Embryos were fixed in 4% paraformaldehyde (PFA) for 4 hours at room temperature and incubated in block for 1 hour. Staining was conducted in PBDT (1% BSA, 1% DMSO, 1% Triton X-100 in PBS), embryos were rinsed for 2 hours, then secondary staining proceeded overnight. Antibodies used were: mouse monoclonal anti-slow-twitch myosin (F59) (Devoto, et al. 1996, generous gift of Frank Stockdale) 1:10, rabbit polyclonal anti-pY^{397}FAK (Biosource, Camarillo, CA) 1:50, mouse monoclonal myosin light chain (F310) (University of Iowa Developmental studies hybridoma bank) 1:10 and rabbit polyclonal anti-β-catenin (Abcam, Cambridge, UK) 1:500. Alexa-Fluor 488, 546, and 633 conjugated goat anti-mouse and goat anti-rabbit secondary antibodies (Invitrogen, Carlsbad, CA) 1:200. Images were acquired using a Leica SP2 confocal microscope and a Zeiss ApoTome running on a Zeiss Axio Imager Z1. For confocal images, embryos were mounted in 100% glycerol and visualized using a 40x oil immersion lens. Image quality was optimized using 2-16 line averaging. Images were processed in Adobe Photoshop and collated in Adobe Illustrator.

Genotyping SBU2

All *SBU2;mib* double mutants and *SBU2* embryos younger than 10 somites are genotyped either after they reach to desired stage and imaged or scored after in-situ hybridization. Genomic DNA is extracted from whole embryos using DNeasy tissue kit (Qiagen, Valencia, CA) or followed the protocol previously described. PCR primers used to genotype *SBU2* embryos are:

Spt6 pvuII F AATGCTGACTGGTTCTCAGCT

Spt6 R2 GCCGCATAATGAAGATCGAC

Following PCR, products were digested with PvuII which cuts the wild-type allele.

Relative quantitation of gene expression by real-time PCR

Total RNA and genomic DNA from single GFP or NICD mRNA injected embryo obtained from SBU2 incross were extracted by using Trizol reagent (Invitrogen, Carlsbad, CA) according to the manufacturer's protocol at 10 somite stage. After each embryo is genotyped, three total RNA preps are pooled and SuperScript II Reverse Transcriptase (Invitrogen, Carlsbad, CA) was used to synthesize first strand cDNA from 0.3 ng of total RNA. Real time PCR was carried out using ABI Prism 7900HT Fast Real-Time PCR system (Applied Biosystems, Foster City, CA) in 15 μL of final volume using 2X FastStart SYBR Green Master (Roche, Indianapolis, IN). Primer pairs used to amplify desired transcripts were:

β-actin: GATTCGCTGGAGATGATG/GTCTTTCTGTCCCATACCAA

her1: AGGCGATTCTAGCAAGGACA/CGAGTTATGGGTTTGGATGG

her6: CCTTGGTAGACTCCGAGGAAA/CGCTGAACAAAGAAAACAAGTG

her7: CAACCAACCTAATCAGAGACGA/ TCTGACAGGCAGTCTGATGG

Total RNA amount of each sample is normalized to relative amount of *β-actin* transcripts in each pool. In each experiment, 3 pools of control and experimental samples were run in duplicates; Ct values of each pool is averaged and relative amounts of gene expression was calculated using relative standard curve prepared for each primer set in each particular real time PCR run.

Acknowledgements

We thank Bernadette Holdener, Peter Gergen, Will Talbot, Keith Gates and Eric Londin for helpful suggestions and comments; Richard Grady, Mihoko Yamamoto and Susanna Li for Fish care; Jack Niemiec for technical assistance. We are also grateful to the many labs that provided reagents and advice, in particular the Yelon laboratory. This work was supported by NIH grant 1RO1HD043998 (HS).

References

Adkins MW, Tyler JK. Transcriptional activators are dispensable for transcription in the absence of Spt6-mediated chromatin reassembly of promoter regions. Mol Cell 2006;21:405–16. [PubMed: 16455495]

Blagden CS, et al. Notochord induction of zebrafish slow muscle mediated by Sonic hedgehog. Genes Dev 1997;11:2163–75. [PubMed: 9303533]

Bortvin A, Winston F. Evidence that Spt6p controls chromatin structure by a direct interaction with histones. Science 1996;272:1473–6. [PubMed: 8633238]

Bray S, et al. Bre1 is required for Notch signaling and histone modification. Dev Cell 2005;8:279–86. [PubMed: 15691768]

Clark-Adams CD, Winston F. The SPT6 gene is essential for growth and is required for delta-mediated transcription in Saccharomyces cerevisiae. Mol Cell Biol 1987;7:679–86. [PubMed: 3029564]

Conlon RA, et al. Notch1 is required for the coordinate segmentation of somites. Development 1995;121:1533–45. [PubMed: 7789282]

Cortes F, et al. Cadherin-mediated differential cell adhesion controls slow muscle cell migration in the developing zebrafish myotome. Dev Cell 2003;5:865–76. [PubMed: 14667409]

Costa PJ, Arndt KM. Synthetic lethal interactions suggest a role for the Saccharomyces cerevisiae Rtf1 protein in transcription elongation. Genetics 2000;156:535–47. [PubMed: 11014804]

Durbin L, et al. Eph signaling is required for segmentation and differentiation of the somites. Genes Dev 1998;12:3096–109. [PubMed: 9765210]

Evrard YA, et al. lunatic fringe is an essential mediator of somite segmentation and patterning. Nature 1998;394:377–81. [PubMed: 9690473]

Forsberg H, et al. Waves of mouse Lunatic fringe expression, in four-hour cycles at two-hour intervals, precede somite boundary formation. Curr Biol 1998;8:1027–30. [PubMed: 9740806]

Gajewski M, et al. Anterior and posterior waves of cyclic her1 gene expression are differentially regulated in the presomitic mesoderm of zebrafish. Development 2003;130:4269–78. [PubMed: 12900444]

Gates MA, et al. A genetic linkage map for zebrafish: comparative analysis and localization of genes and expressed sequences. Genome Res 1999;9:334–47. [PubMed: 10207156]

Gray M, et al. Zebrafish deadly seven functions in neurogenesis. Dev Biol 2001;237:306–23. [PubMed: 11543616]

Greenwald I. LIN-12/Notch signaling: lessons from worms and flies. Genes Dev 1998;12:1751–62. [PubMed: 9637676]

Hartzog GA, et al. Evidence that Spt4, Spt5, and Spt6 control transcription elongation by RNA polymerase II in Saccharomyces cerevisiae. Genes Dev 1998;12:357–69. [PubMed: 9450930]

Henry CA, Amacher SL. Zebrafish slow muscle cell migration induces a wave of fast muscle morphogenesis. Dev Cell 2004;7:917–23. [PubMed: 15572133]

Henry CA, et al. Roles for zebrafish focal adhesion kinase in notochord and somite morphogenesis. Dev Biol 2001;240:474–87. [PubMed: 11784077]

Henry CA, et al. Somites in zebrafish doubly mutant for knypek and trilobite form without internal mesenchymal cells or compaction. Curr Biol 2000;10:1063–6. [PubMed: 10996075]

Henry CA, et al. Interactions between muscle fibers and segment boundaries in zebrafish. Dev Biol 2005;287:346–60. [PubMed: 16225858]

Henry CA, et al. Two linked hairy/Enhancer of split-related zebrafish genes, her1 and her7, function together to refine alternating somite boundaries. Development 2002;129:3693–704. [PubMed: 12117818]

Hens MD, DeSimone DW. Molecular analysis and developmental expression of the focal adhesion kinase pp125FAK in Xenopus laevis. Dev Biol 1995;170:274–88. [PubMed: 7649362]

Holley SA, et al. Control of her1 expression during zebrafish somitogenesis by a delta-dependent oscillator and an independent wave-front activity. Genes Dev 2000;14:1678–90. [PubMed: 10887161]

Holley SA, et al. her1 and the notch pathway function within the oscillator mechanism that regulates zebrafish somitogenesis. Development 2002;129:1175–83. [PubMed: 11874913]

Hrabe de Angelis M, et al. Maintenance of somite borders in mice requires the Delta homologue DII1. Nature 1997;386:717–21. [PubMed: 9109488]

Hubbard EJ, et al. Evidence for physical and functional association between EMB-5 and LIN-12 in Caenorhabditis elegans. Science 1996;273:112–5. [PubMed: 8658178]

Itoh M, et al. Mind bomb is a ubiquitin ligase that is essential for efficient activation of Notch signaling by Delta. Dev Cell 2003;4:67–82. [PubMed: 12530964]

Jiang YJ, et al. Notch signalling and the synchronization of the somite segmentation clock. Nature 2000;408:475–9. [PubMed: 11100729]

Jiang YJ, et al. Mutations affecting neurogenesis and brain morphology in the zebrafish, Danio rerio. Development 1996;123:205–16. [PubMed: 9007241]

Julich D, et al. beamter/deltaC and the role of Notch ligands in the zebrafish somite segmentation, hindbrain neurogenesis and hypochord differentiation. Dev Biol 2005;286:391–404. [PubMed: 16125692]

Kaplan CD, et al. Transcription elongation factors repress transcription initiation from cryptic sites. Science 2003;301:1096–9. [PubMed: 12934008]

Kaplan CD, et al. Spt5 and spt6 are associated with active transcription and have characteristics of general elongation factors in D. melanogaster. Genes Dev 2000;14:2623–34. [PubMed: 11040216]

Keegan BR, et al. The elongation factors Pandora/Spt6 and Foggy/Spt5 promote transcription in the zebrafish embryo. Development 2002;129:1623–32. [PubMed: 11923199]

Kim CH, et al. Zebrafish elav/HuC homologue as a very early neuronal marker. Neurosci Lett 1996;216:109–12. [PubMed: 8904795]

Kimmel CB, et al. Stages of embryonic development of the zebrafish. Dev Dyn 1995;203:253–310. [PubMed: 8589427]

Krauss S, et al. Expression of the zebrafish paired box gene pax[zf-b] during early neurogenesis. Development 1991;113:1193–206. [PubMed: 1811936]

Kusumi K, et al. The mouse pudgy mutation disrupts Delta homologue Dll3 and initiation of early somite boundaries. Nat Genet 1998;19:274–8. [PubMed: 9662403]

Malone EA, et al. Molecular and genetic characterization of SPT4, a gene important for transcription initiation in Saccharomyces cerevisiae. Mol Gen Genet 1993;237:449–59. [PubMed: 8483459]

McGrew MJ, et al. The lunatic fringe gene is a target of the molecular clock linked to somite segmentation in avian embryos. Curr Biol 1998;8:979–82. [PubMed: 9742402]

Nikaido M, et al. Tbx24, encoding a T-box protein, is mutated in the zebrafish somite-segmentation mutant fused somites. Nat Genet 2002;31:195–9. [PubMed: 12021786]

Nishiwaki K, et al. emb-5, a gene required for the correct timing of gut precursor cell division during gastrulation in Caenorhabditis elegans, encodes a protein similar to the yeast nuclear protein SPT6. Mol Gen Genet 1993;239:313–22. [PubMed: 8391108]

Oates AC, Ho RK. Hairy/E(spl)-related (Her) genes are central components of the segmentation oscillator and display redundancy with the Delta/Notch signaling pathway in the formation of anterior segmental boundaries in the zebrafish. Development 2002;129:2929–46. [PubMed: 12050140]

Oka C, et al. Disruption of the mouse RBP-J kappa gene results in early embryonic death. Development 1995;121:3291–301. [PubMed: 7588063]

Oxtoby E, Jowett T. Cloning of the zebrafish krox-20 gene (krx-20) and its expression during hindbrain development. Nucleic Acids Res 1993;21:1087–95. [PubMed: 8464695]

Pawson T. Protein modules and signalling networks. Nature 1995;373:573–80. [PubMed: 7531822]

Polte TR, et al. Focal adhesion kinase is abundant in developing blood vessels and elevation of its phosphotyrosine content in vascular smooth muscle cells is a rapid response to angiotensin II. J Cell Biochem 1994;55:106–19. [PubMed: 7521880]

Pourquie O. Vertebrate somitogenesis. Annu Rev Cell Dev Biol 2001;17:311–50. [PubMed: 11687492]

Pourquie O. The segmentation clock: converting embryonic time into spatial pattern. Science 2003;301:328–30. [PubMed: 12869750]

Saunders A, et al. Tracking FACT and the RNA polymerase II elongation complex through chromatin in vivo. Science 2003;301:1094–6. [PubMed: 12934007]

Schier AF, et al. Mutations affecting the development of the embryonic zebrafish brain. Development 1996;123:165–78. [PubMed: 9007238]

Sirotkin HI, et al. bozozok and squint act in parallel to specify dorsal mesoderm and anterior neuroectoderm in zebrafish. Development 2000;127:2583–92. [PubMed: 10821757]

Swanson MS, Winston F. SPT4, SPT5 and SPT6 interactions: effects on transcription and viability in Saccharomyces cerevisiae. Genetics 1992;132:325–36. [PubMed: 1330823]

Takke C, Campos-Ortega JA. her1, a zebrafish pair-rule like gene, acts downstream of notch signalling to control somite development. Development 1999;126:3005–14. [PubMed: 10357943]

Takke C, et al. her4, a zebrafish homologue of the Drosophila neurogenic gene E(spl), is a target of NOTCH signalling. Development 1999;126:1811–21. [PubMed: 10101116]

Tenney K, et al. Drosophila Rtf1 functions in histone methylation, gene expression, and Notch signaling. Proc Natl Acad Sci U S A 2006;103:11970–4. [PubMed: 16882721]

Thisse C, et al. Structure of the zebrafish snail1 gene and its expression in wild-type, spadetail and no tail mutant embryos. Development 1993;119:1203–15. [PubMed: 8306883]

Topczewska JM, et al. The winged helix transcription factor Foxc1a is essential for somitogenesis in zebrafish. Genes Dev 2001;15:2483–93. [PubMed: 11562356]

Tsai SF, et al. Cloning of cDNA for the major DNA-binding protein of the erythroid lineage through expression in mammalian cells. Nature 1989;339:446–51. [PubMed: 2725678]

Tsukiyama T, Wu C. Chromatin remodeling and transcription. Curr Opin Genet Dev 1997;7:182–91. [PubMed: 9115421]

van Eeden FJ, et al. Mutations affecting somite formation and patterning in the zebrafish, Danio rerio. Development 1996;123:153–64. [PubMed: 9007237]

Weinberg ES, et al. Developmental regulation of zebrafish MyoD in wild-type, no tail and spadetail embryos. Development 1996;122:271–80. [PubMed: 8565839]

Winkler M, et al. Functional interaction between pleiotropic transactivator pUL69 of human cytomegalovirus and the human homolog of yeast chromatin regulatory protein SPT6. J Virol 2000;74:8053–64. [PubMed: 10933715]

Wong PC, et al. Presenilin 1 is required for Notch1 and DII1 expression in the paraxial mesoderm. Nature 1997;387:288–92. [PubMed: 9153393]

Wood A, et al. The Paf1 complex is essential for histone monoubiquitination by the Rad6-Bre1 complex, which signals for histone methylation by COMPASS and Dot1p. J Biol Chem 2003;278:34739–42. [PubMed: 12876294]

Yamamoto A, et al. Zebrafish paraxial protocadherin is a downstream target of spadetail involved in morphogenesis of gastrula mesoderm. Development 1998;125:3389–97. [PubMed: 9693142]

Zhang N, Gridley T. Defects in somite formation in lunatic fringe-deficient mice. Nature 1998;394:374–7. [PubMed: 9690472]

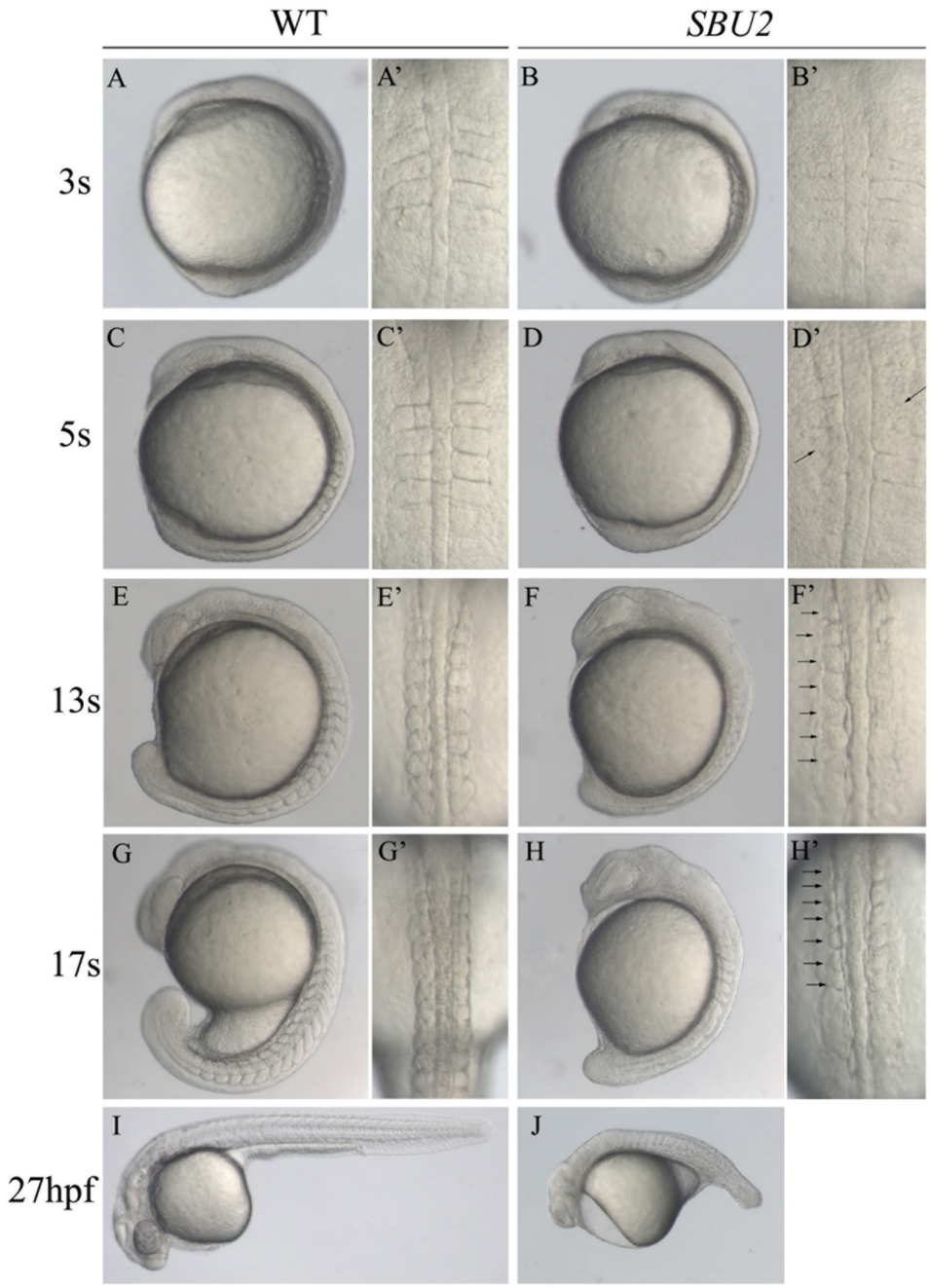

Figure 1.

Phenotype of *SBU2* mutants. (A-J) Lateral views of living WT and SBU2 embryos, anterior to the top and dorsal to the right. (A'-H') Dorsal views of A-H, anterior to the top. At early somitogenesis, somite boundaries are irregular and indefinite (A' and B') in *SBU2* embryos. At ~5 somite stage, somites are formed asymmetrically while previously formed somite boundaries start to degenerate (arrows) (C' and D'). By the 5-somite stage SBU2 mutants have a slightly shorter body length then their wild-type siblings (C and D) and by 13 somite stage, *SBU2* mutants are clearly less extended along AP axis than wild type embryos (E and F). While somites continue to form in wild-type embryos, *SBU2* mutants have only irregularly formed 6-7 somites and lack posterior somites (arrows) (F' and H'). By 24-27 hpf, most of the

previously formed structures including somite boundaries are degraded or distorted and the embryos degenerate (J). Note: all of the embryos shown in this figure and the following figures are diploids.

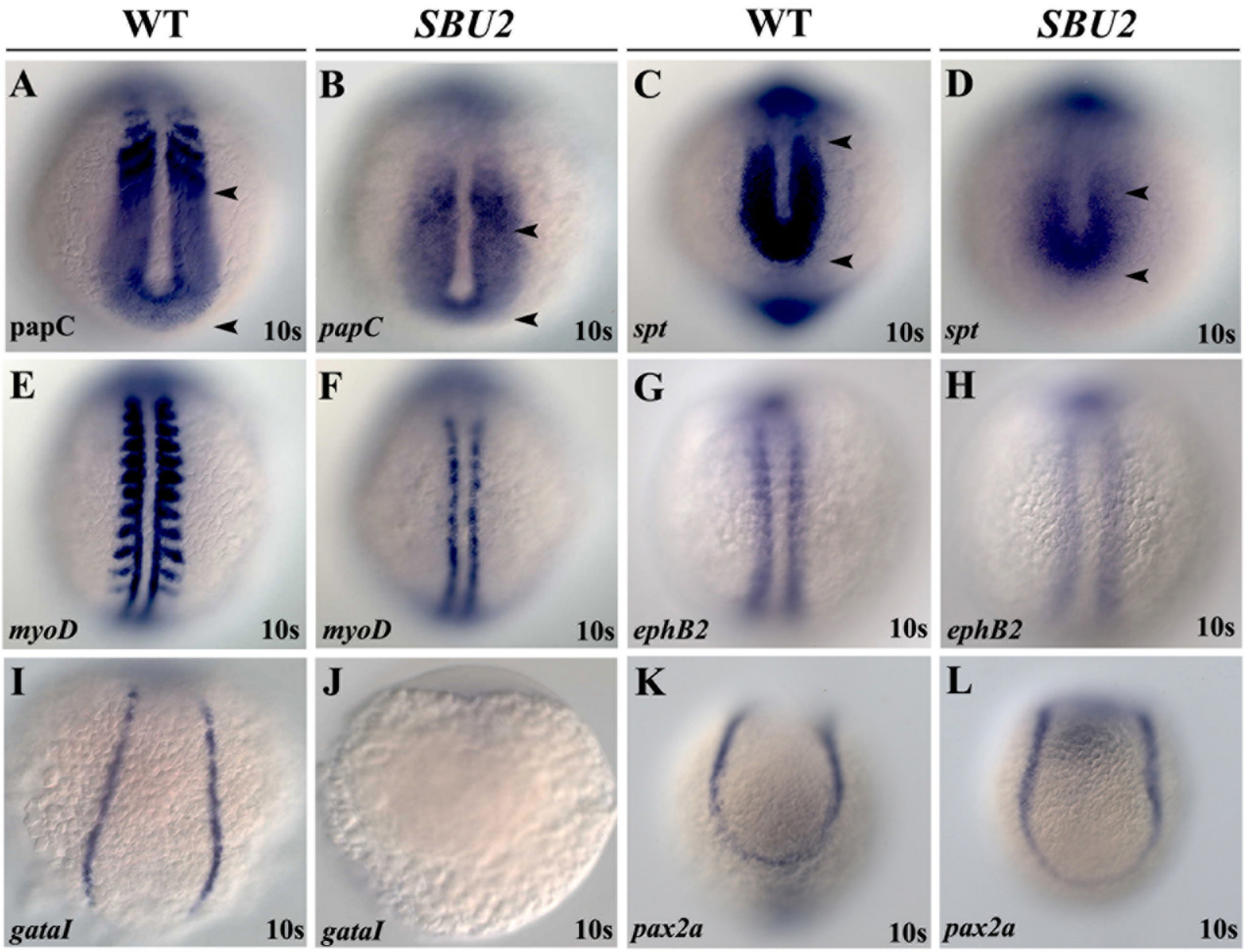

Figure 2.

SBU2 mutants have mesoderm defects. Whole mount RNA in situ hybridization of mesodermal markers in wild-type and *SBU2* mutants. All views are dorsal; anterior to the top. The expression domains of presomitic mesoderm markers *papC* and s*pt* are reduced in *SBU2* mutants (A-D). AP patterning of the somites in *SBU2* embryos is also affected; *myoD* expression at the posterior half of the somites is lost while it is reduced at adaxial cells (E and F), *ephB2* at the anterior half of the somites is reduced and more diffused (G and H). *gataI* expression is diminished in *SBU2* mutants (I and J) indicating that lateral plate mesoderm development is highly reduced. There is no apparent difference in *pax2a* expression between wild type and *SBU2* mutants (K and L); *SBU2* mutants have no defect in intermediate mesoderm formation. The most anterior and posterior *papC* and s*pt* expression is marked by arrowheads.

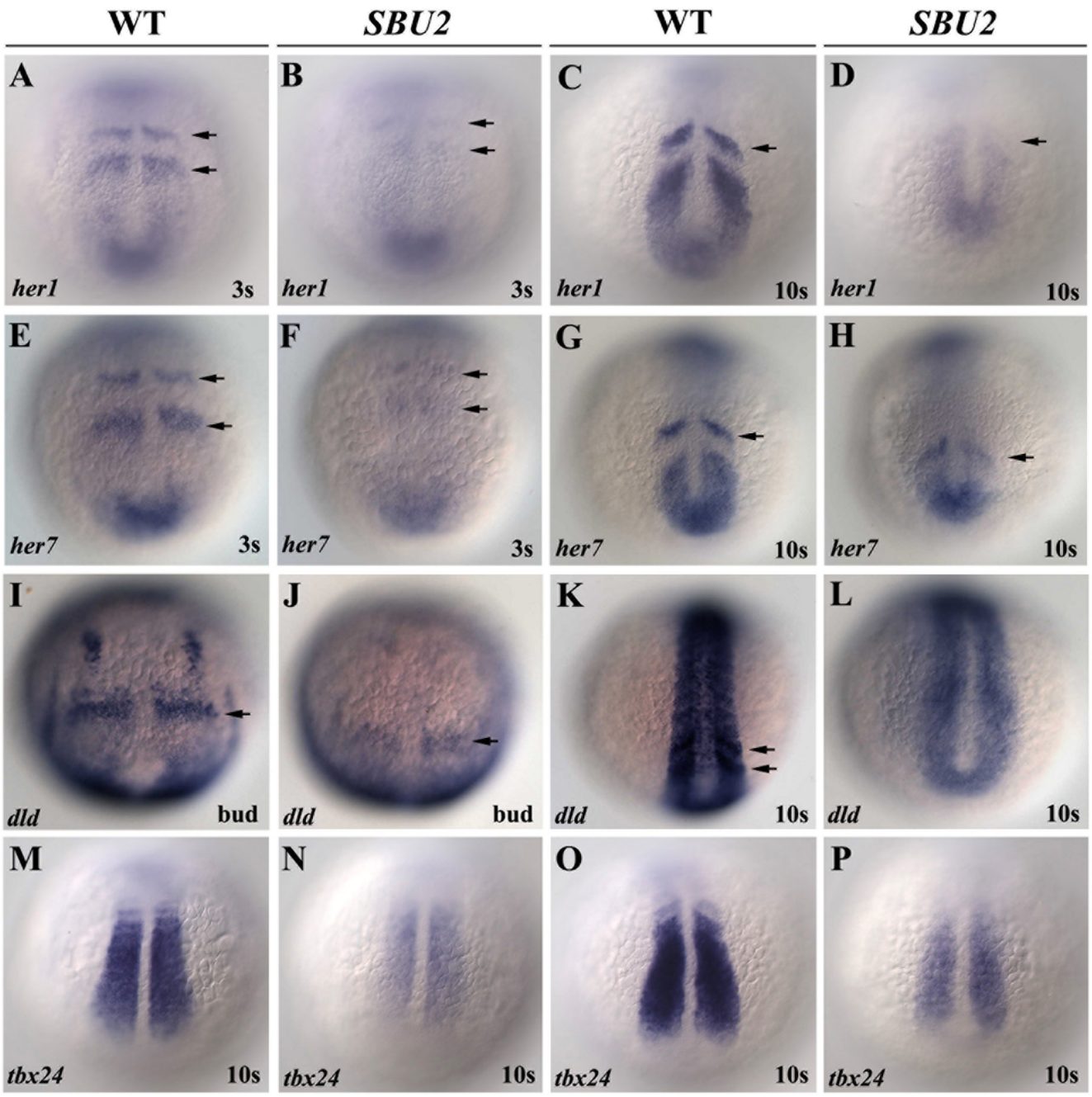

Figure 3.

Somite segmentation and PSM maturation is disrupted in *SBU2* mutants. Whole mount RNA in situ hybridization of genes involved in somite segmentation process in wild-type and *SBU2* mutants. All views are dorsal; anterior to the top. In wild type embryos, periodic activation of notch signaling provides cycling gene expression of Notch pathway genes such as *her1* and *her7* (A-D and E-H). *dld* expression is weak and diffused in presomitic mesoderm as well as anteriormost somites (I-L). *tbx24*, normally expressed in intermediate and anterior PSM, is also reduced in *SBU2* embryos (M-P). Arrows denote stripes of *her1*, *her7* or *dld* expression.

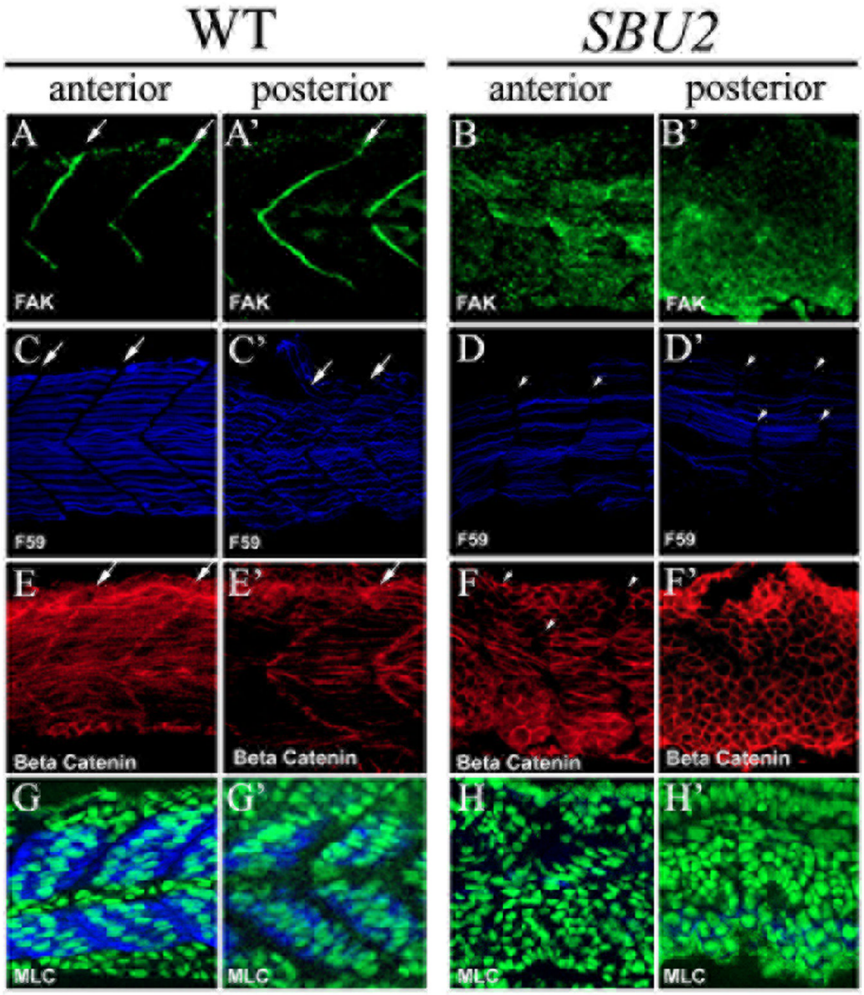

Figure 4.

Somite boundary formation and muscle fiber differentiation is disrupted in *SBU2* mutants. Confocal sections of anterior (A-H) and posterior (A'-H') portions of the trunk region 29 somite stage embryos at approximately same medial-lateral and anterior-posterior locations; anterior to the left. Focal adhesion marker phosphorylated Fak is in green; slow muscle marker F59 is in blue; β-catenin which outlines the cell is in red. In wild type embryos, phosphorylated Fak accumulates at myotome borders, revealing regularly formed somite boundaries (A and A'). On the other hand, there is no specific accumulation of phosphorylated FAK in *SBU2* mutants (B and B'). The number of the slow muscle fibers is lower both in anterior and posterior (D and D') compared to wild type muscle fibers (C and C'). In wild-type embryos, fast muscle precursors elongate and attach to the anterior and posterior somite borders (E). In *SBU2* mutant embryos, some fast cells elongate in the anterior of the embryos (F). However, in the posterior, few, if any, fast cells elongate (F'). Likewise, the MLC antibody F310 staining (blue) is abundant in wild-type muscle (G and G') but absent in SBU2 mutant embryos (H and H'), nuclei are labeled with cytoxgreen. Therefore, fast muscle fiber morphogenesis is severely disrupted in *SBU2* mutant embryos. Arrows denote somite boundaries. Arrowheads denote improper and degenerated somite boundaries.

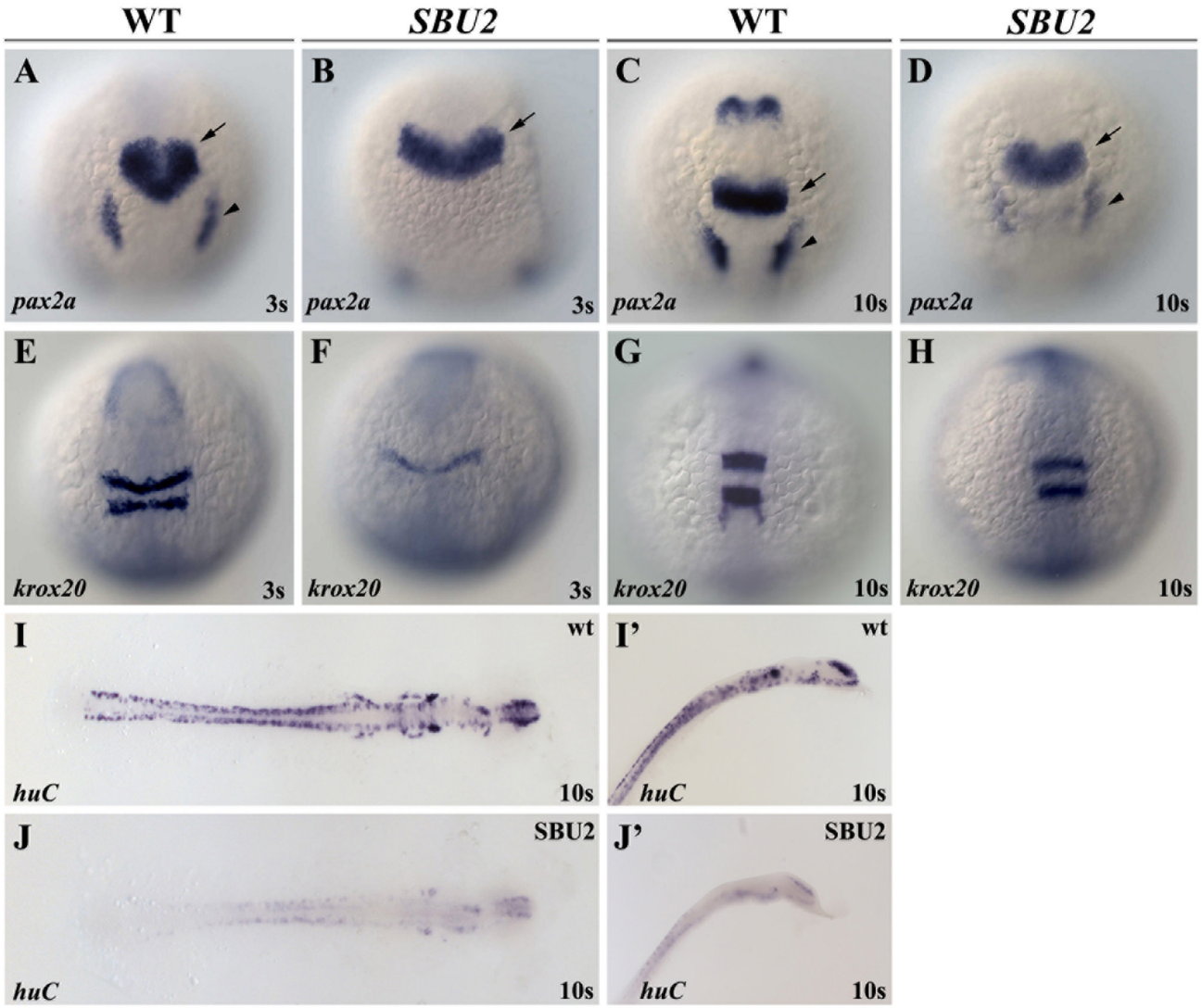

Figure 5.

SBU2 mutants are not neurogenic. Whole mount RNA in situ hybridization of neural markers in wild-type and *SBU2* mutants. (A-J) Dorsal views; (A-H) anterior to the top, (I, J) flat mounted, anterior to the right. I', J' are lateral views of I and J, anterior to the top right. Morphology of the MHB domain expressing *pax2a* at early somitogenesis (B) indicates a delay in development of MHB in *SBU2* mutants. Later, at 10 somite stage (D) *pax2a* expression resembles much earlier stage wild type expression domain (A). Likewise, although hindbrain marker *krox20* expression is also delayed and relatively reduced (E and F) later in the development, expression pattern appears similar to wild-type embryos (G and H). RNA *in situ* hybridization using *huC* probe revealed that *SBU2* embryos have reductions in early differentiating neurons (I, I' and J, J'). Arrows denote MHB and arrowheads denote otic placode.

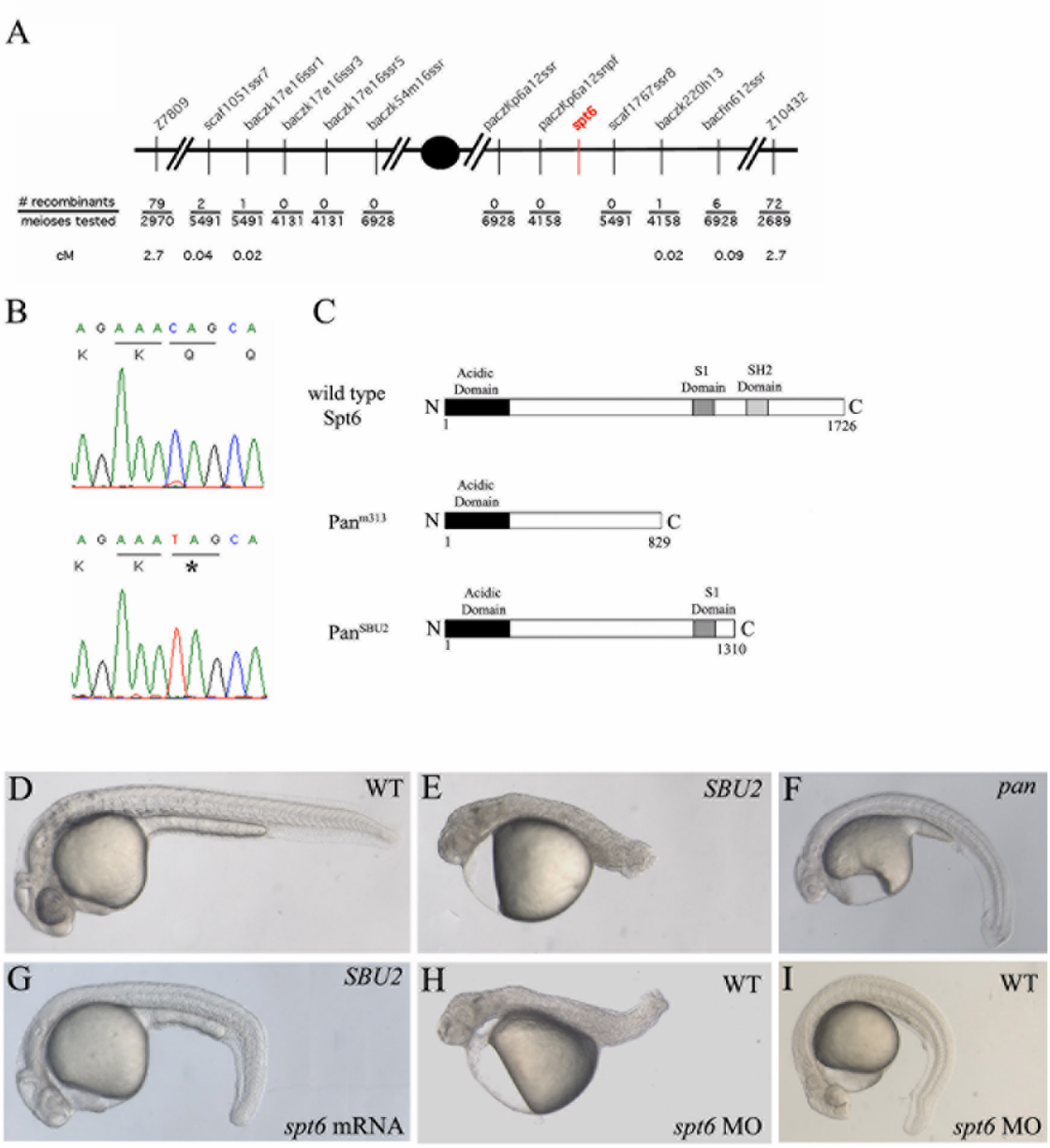

Figure 6.

SBU2 phenotype is the result of a non-sense mutation on *spt6* gene. *SBU2* maps to linkage group 21 between Z7809 and Z10432 (A). Sequencing analysis revealed a C to T transition at the 3931st nucleotide of the coding sequence of the *spt6* gene (B). Predicted Spt6 protein structure in wild type, *pan*^{m313} and *pan*^{SBU2} mutant embryos (C). The premature stop codon in *SBU2* is predicted to produce a truncated protein which lacks SH2 domain (C). The defects in homozygous *SBU2* embryos can be rescued by injection of *spt6* mRNA (G). Microinjection of *spt6* morpholino into the progeny from intercrosses of wild-type siblings of *SBU2* heterozygotes, phenocopies *SBU2* mutants (H). However, in some wild type stocks, the phenotype upon injection of *spt6* morpholino is much weaker (I) and resembles *pan* phenotype (F). (D, E, G, H) are 27-hour-old; (F and I) are 48-hour old embryos. Asterisk denotes stop codon in (B).

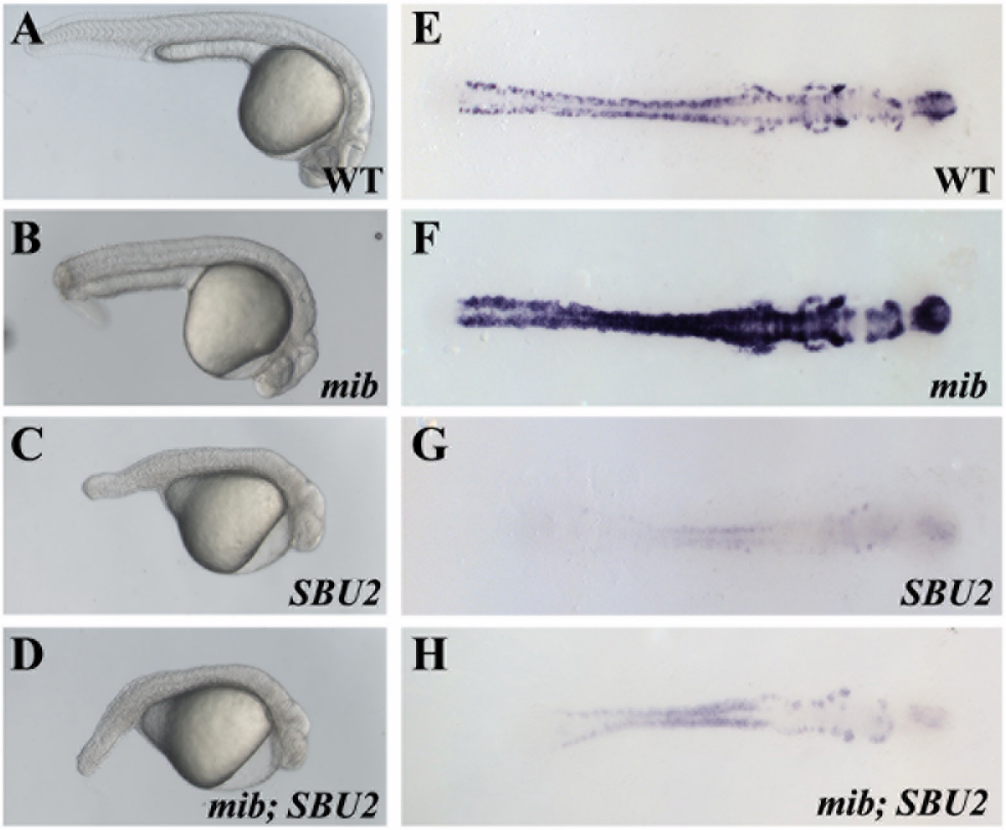

Figure 7.

Spt6 genetically interacts with Notch1a. (A-D) Activation of Notch pathway was monitored by the relative quantification of transcripts of Notch pathway target genes. The intracellular domain of Notch1a (NICD) was injected to 1-4 cell stage embryos obtained from SBU2 incross; cDNA synthesized from total RNA pools from 10 somite embryos were used for real time PCR. Each set of data is normalized to transcript level from the GFP injected wild type siblings. Bars represent means of measurements from three different mRNA pools. Standard error of the mean is also shown. Levels of *her1*, *her6* and *her7* transcripts are increased when Notch pathway is activated via NICD injection (third bar in A, B, C). Transcripts of Notch pathway target genes are reduced in SBU2 mutants. (second bar in A, B, C). However, *SBU2* mutation impedes activation of Notch pathway upon NICD injection; *her1*, *her6* and *her7* transcript levels stay relatively lower with respect to transcript levels in NICD injected wild type siblings (compare third and fourth bar in A, B, C) when Spt6 gene is disrupted in NICD injected embryos.

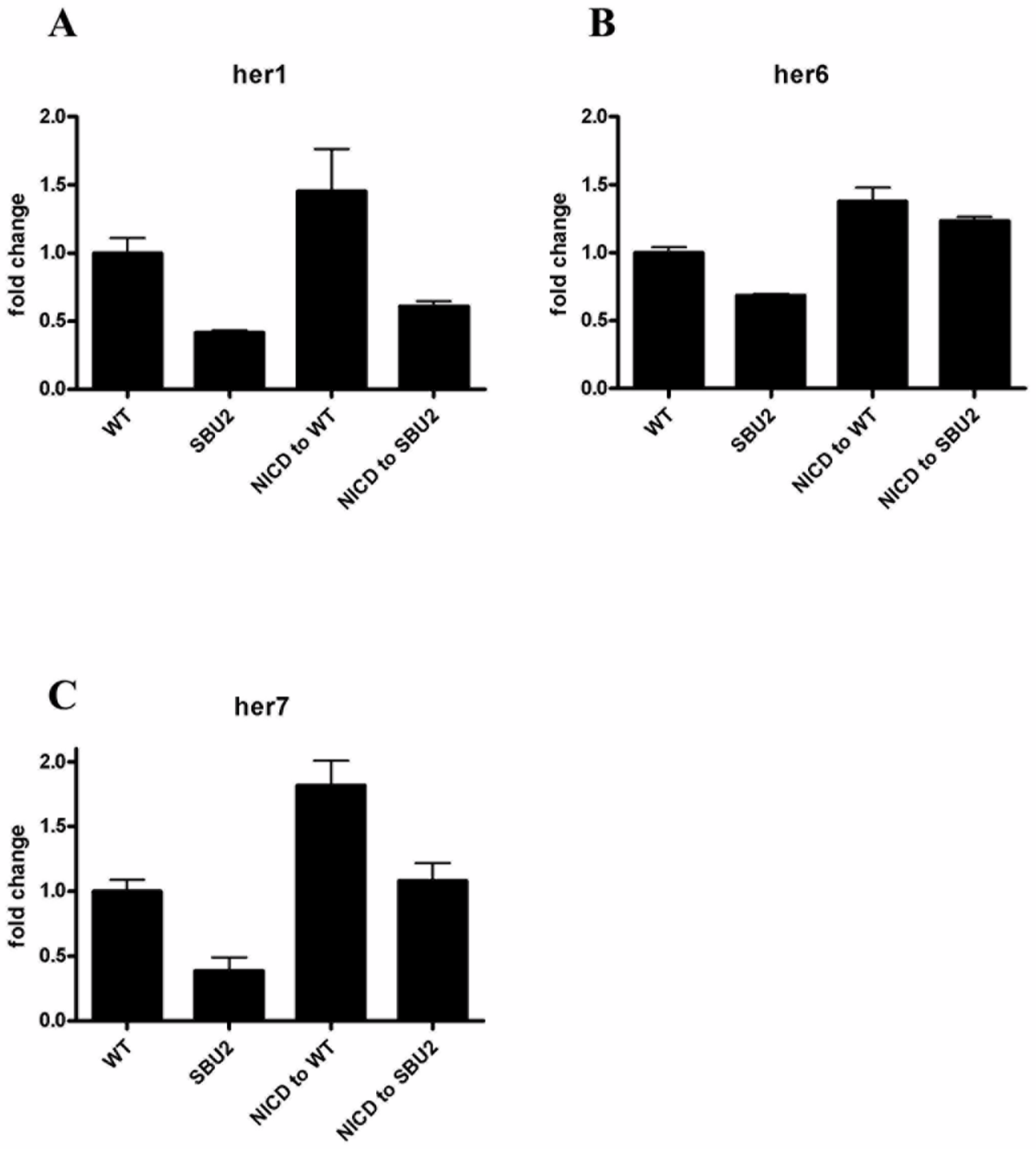

Figure 8.

mib; SBU2 double mutants reveal an epistatic interaction between Spt6 and Notch pathway. (A-D) Lateral views of 27 hour-old embryos, anterior to the right. (E-H) Dorsal views of *huC* stained embryos, anterior to the right. All embryos were genotyped following photography. The phenotype of *mib; SBU2* mutants (D) resembles *SBU2* single mutants (C), rather than *mib* single mutant embryos (B). However, *huC* expression profile in *mib; SBU2* double mutants (H) is stronger than *SBU2* mutants (G) but not as strong as either wild type (E) or *mib* single mutants (F).